



**HAL**  
open science

## De novo structure determination of 3-((3-aminopropyl)amino)- 4-hydroxybenzoic acid, a novel and abundant metabolite in *Acinetobacter baylyi* ADP1

Marion Thomas, Lucille Stuani, Ekaterina Darii, Christophe Lechaplais,  
Emilie Pateau, Jean-Claude Tabet, Marcel Salanoubat, Pierre-Loïc Saaidi,  
Alain Perret

### ► To cite this version:

Marion Thomas, Lucille Stuani, Ekaterina Darii, Christophe Lechaplais, Emilie Pateau, et al.. De novo structure determination of 3-((3-aminopropyl)amino)- 4-hydroxybenzoic acid, a novel and abundant metabolite in *Acinetobacter baylyi* ADP1. *Metabolomics*, 2019, 15, pp.45. 10.1007/s11306-019-1508-3 . hal-02323597

**HAL Id: hal-02323597**

**<https://hal.science/hal-02323597v1>**

Submitted on 22 Oct 2019

**HAL** is a multi-disciplinary open access archive for the deposit and dissemination of scientific research documents, whether they are published or not. The documents may come from teaching and research institutions in France or abroad, or from public or private research centers.

L'archive ouverte pluridisciplinaire **HAL**, est destinée au dépôt et à la diffusion de documents scientifiques de niveau recherche, publiés ou non, émanant des établissements d'enseignement et de recherche français ou étrangers, des laboratoires publics ou privés.



2 **De novo structure determination of 3-((3-aminopropyl)amino)-**  
3 **4-hydroxybenzoic acid, a novel and abundant metabolite**  
4 **in *Acinetobacter baylyi* ADP1**

5 Marion Thomas<sup>1</sup> · Lucille Stuani<sup>2</sup> · Ekaterina Darii<sup>1</sup> · Christophe Lechaplais<sup>1</sup> · Emilie Pateau<sup>1</sup> ·  
6 Jean-Claude Tabet<sup>3,4</sup> · Marcel Salanoubat<sup>1</sup> · Pierre-Loïc Saaidi<sup>1</sup> · Alain Perret<sup>1</sup>

7 Received: 4 October 2018 / Accepted: 7 March 2019  
8 © Springer Science+Business Media, LLC, part of Springer Nature 2019

9 **Abstract**

10 **Introduction** Metabolite identification remains a major bottleneck in the understanding of metabolism. Many metabolomics **AQ1**  
11 studies end up with unknown compounds, leaving a landscape of metabolites and metabolic pathways to be unraveled.  
12 Therefore, identifying novel compounds within a metabolome is an entry point into the ‘dark side’ of metabolism.

13 **Objectives** This work aimed at elucidating the structure of a novel metabolite that was first detected in the soil bacterium **AQ2**  
14 *Acinetobacter baylyi* ADP1 (ADP1).

15 **Methods** We used high resolution multi-stage tandem mass spectrometry for characterizing the metabolite within the  
16 metabolome. We purified the molecule for 1D- and 2D-NMR (<sup>1</sup>H, <sup>13</sup>C, <sup>1</sup>H-<sup>1</sup>H-COSY, <sup>1</sup>H-<sup>13</sup>C-HSQC, <sup>1</sup>H-<sup>13</sup>C-HMBC and  
17 <sup>1</sup>H-<sup>15</sup>N-HMBC) analyses. Synthetic standards were chemically prepared from MS and NMR data interpretation.

18 **Results** We determined the de novo structure of a previously unreported metabolite: 3-((3-aminopropyl)amino)-4-hydroxy-  
19 benzoic acid. The proposed structure was validated by comparison to a synthetic standard. With a concentration in the mil-  
20 limolar range, this compound appears as a major metabolite in ADP1, which we anticipate to participate to an unsuspected  
21 metabolic pathway. This novel metabolite was also detected in another  $\gamma$ -proteobacterium.

22 **Conclusion** Structure elucidation of this abundant and novel metabolite in ADP1 urges to decipher its biosynthetic pathway  
23 and cellular function.

24 **Keywords** Functional genomics · Bacterial metabolism · LC/MS-orbitrap · NMR · Structure elucidation

A1 Marion Thomas and Lucille Stuani have contributed equally to this  
A2 work.

A3 **Electronic supplementary material** The online version of this  
A4 article (<https://doi.org/10.1007/s11306-019-1508-3>) contains  
A5 supplementary material, which is available to authorized users.

A6 ✉ Pierre-Loïc Saaidi  
A7 plsaaidi@genoscope.cns.fr

A8 ✉ Alain Perret  
A9 aperret@genoscope.cns.fr

A10 <sup>1</sup> Génomique Métabolique, Genoscope, Institut François  
A11 Jacob, CEA, CNRS, Univ Evry, Université Paris-Saclay,  
A12 91057 Evry, France

A13 <sup>2</sup> INSERM, Institut National de la Santé et de la Recherche  
A14 Médicale - CNRS - UPS - Centre de Recherche en  
A15 Cancérologie de Toulouse (CRCT), Toulouse, France

A16 <sup>3</sup> Sorbonne Université, UPMC Univ Paris 06, CNRS, Institut  
A17 Parisien de Chimie Moléculaire, Paris, France

A18 <sup>4</sup> CEA, iBiTec-S, SPI, LEMM, Gif-sur-Yvette, France

## 1 Introduction

25  
26 Extensive and accurate knowledge of bacterial metabolism  
27 is critical for developing a comprehensive and detailed  
28 understanding of cellular physiology. This requires that, *in*  
29 *fine*, within a studied organism the function of all genes is  
30 established and the identity of all metabolites known. This  
31 goal is today probably out of reach given the complexity  
32 of the chemistry of life, and represents a long-term objec-  
33 tive. On the one side 30–40% of genes of a typical genome  
34 remain unannotated or associated with a putative function  
35 (Chang et al. 2016; Galperin and Koonin 2004) and on  
36 the other side, many metabolites remain unidentified in  
37 most metabolomics studies (Bingol et al. 2016; Dias et al.  
38 2016; Domingo-Almenara et al. 2018; Dunn et al. 2013b;  
39 Viant et al. 2017). Nuclear magnetic resonance (NMR)  
40 is currently the most powerful spectroscopic method for  
41 elucidating the chemical structure of organic compounds

due to the development of high field magnets as well as capillary and cryogenic probes that significantly increased the sensitivity of NMR spectroscopy (Dias et al. 2016). However, this technique most preferably needs a pure sample in the upper  $\mu\text{M}$  range that requires laborious and time consuming work. Moreover, since annotating compounds to most likely structures using high-resolution mass spectrometry (HRMS) is a faster and feasible first step, electrospray-mass spectrometry (ESI-MS) and tandem mass spectrometry combined with liquid chromatographic (LC) separation is the most used technique for characterizing unknown compounds present in metabolomes. Nevertheless, many metabolomic studies end up with a mere list of mass-to-charge ratio ( $m/z$ ) values and chromatographic retention times. As a consequence, a landscape of metabolites and metabolic pathways are yet to be discovered. In metabolomics, identification of metabolites remains one of the biggest bottlenecks (Dunn et al. 2013a; Kind and Fiehn 2010; Viant et al. 2017), but of importance, since identifying novel compounds within a metabolome is an entry point into the ‘dark side’ of bacterial metabolism. The use of HRMS instruments with mass accuracy in the low parts per million (ppm) range can provide the elemental composition of the detected ions. HRMS also provides a useful method for putative annotation querying databases (Kanehisa et al. 2012; Smith et al. 2005; Wishart et al. 2013) for metabolites whose molecular masses are within a specified mass deviation range. However, the majority of the observed peaks continue to remain unidentified or associated with multiple putative identifications. Without authentic compounds used for comparison of retention time and product ion spectra, the identity of a metabolite cannot be established. Structural information can also be obtained by performing MS/MS experiments, where the ion is fragmented and the  $m/z$  of the resulting fragment ions recorded. However, fragmentation interpretation of an unknown metabolite for its structural elucidation remains hampered by our incomplete understanding of the complex gas phase ion chemistry. Alternatively, these spectra can be matched with existing spectral databases for identity assignment or similarity search (Zhu et al. 2013). These databases, which are increasing in number and size (Horai et al. 2010; <https://www.mzcloud.org>; Kale et al. 2016; Sawada et al. 2012; Smith et al. 2005; Wishart et al. 2013) are very useful for identifying known compounds, but are far from being complete. Only a small proportion of all known metabolites are commercially available, leaving the majority of them not included in mass spectral libraries. It is estimated that less than 5% of all known metabolites are MS<sup>2</sup> spectra available (Frainay et al. 2018; Tsugawa et al. 2016). Another drawback of ESI-MS/MS experiments is that the tandem mass spectra generated exhibit high instrument-dependent variability which interferes with the

constitution of universal databases as done with electron ionization mass spectrometry (Roux et al. 2011). Compared to MS<sup>2</sup> approaches, multistage MS (MS<sup>n</sup>) fragmentation in which ions are specifically selected for sequential fragmentation, results in deeper and more detailed fragmentation pathways and provides more structural information (Rojas-Cherto et al. 2012; van der Hooft et al. 2011). In this case, again, complete identification is possible only when a fragmentation tree of the same compound is present in the database. Otherwise, putative candidate structures can be proposed using computer assisted structure elucidation (Peironcelly et al. 2012; Wolf et al. 2010) but the identity of the unknown remains non-validated. Four levels of reporting metabolite annotation and identification are defined by the metabolomics standards initiative (Sumner et al. 2007). ‘‘Identification’’ is the most rigorous level (level 1), where two orthogonal properties of the metabolite are matched to the same properties of an authentic compound analyzed by the same method. Levels 2 and 3 provide annotation as metabolites or metabolite classes, respectively, without comparison to authentic compounds. Level 4 considers the metabolite as unidentified. Therefore, only information from rigorously ‘level 1’ identified metabolites can be used for investigating metabolic pathways and accessing other levels of biological hierarchy such as gene function annotation.

*Acinetobacter baylyi* ADP1 (ADP1) is a nutritionally versatile strictly aerobic bacterium (Young et al. 2005). Its extraordinary competence for natural transformation and the ease with which it can be genetically engineered (de Berardinis 2009; Metzgar et al. 2004) make ADP1 a key organism for the study of bacterial metabolism. We recently used metabolomics to reinvestigate quinate metabolism in ADP1, which was thoroughly studied for many years (Young et al. 2005). We reported that shifting the carbon source from succinate to quinate elicited a global metabolic reprogramming and led to the production of almost 30 unidentified and unexpected compounds that we anticipate to participate to unsuspected metabolic pathways (Stuani et al. 2014). Here, we report the complete de novo structure elucidation of one these unknown metabolites. We conducted its extensive LC/HRMS/MS<sup>n</sup> characterization within the metabolome and purified the molecule for 1D- and 2D-NMR (<sup>1</sup>H, <sup>13</sup>C, <sup>1</sup>H-<sup>1</sup>H-COSY, <sup>1</sup>H-<sup>13</sup>C-HSQC, <sup>1</sup>H-<sup>13</sup>C-HMBC and <sup>1</sup>H-<sup>15</sup>N-HMBC) analyses. The putative structure deduced from MS and NMR data interpretation was eventually confirmed by means of chemical synthesis to be 3-((3-aminopropyl) amino)-4-hydroxybenzoic acid (APAH). This compound was discovered to be a major metabolite in ADP1 with intracellular concentration in the millimolar range. Its presence in another  $\gamma$ -proteobacterium such as *Pseudomonas putida* suggests a wider taxonomic distribution and urges to investigate its metabolic role.

## 148 2 Materials and methods

### 149 2.1 Chemicals and reagents

150 Chemicals, HPLC-grade solvents, ammonium acetate,  
151 ammonium carbonate, ammonium hydroxide and deuter-  
152 ated water were from Sigma-Aldrich. 5-((3-aminopropyl)  
153 amino)-2-hydroxybenzoic acid (SN0079), 4-((3-aminopro-  
154 pyl)amino)-2-hydroxybenzoic acid (SN0080), 2-((3-amino-  
155 propyl)amino)-5-hydroxybenzoic acid (SN0123), 4-((3-amino-  
156 propyl)amino)-3-hydroxybenzoic acid (SN0124) and  
157 3-((3-aminopropyl)amino)-4-hydroxybenzoic acid (SN0140)  
158 were synthesized by Synthenova ([http://www.synthenova](http://www.synthenova.com)  
159 [.com](http://www.synthenova.com)).

### 160 2.2 Strains and medium

161 *Acinetobacter baylyi* ADP1 strain (DSM 24193) was pro-  
162 vided by Dr. Nicholas Ornston (Yale University). ADP1,  
163 *Pseudomonas putida* KT2440 (ATCC 47054) and *Ralsto-*  
164 *nia eutropha* H16 (DSMZ 428) were routinely grown on  
165 medium for *Acinetobacter* (MA) minimal medium [31 mM  
166 Na<sub>2</sub>HPO<sub>4</sub>, 25 mM KH<sub>2</sub>PO<sub>4</sub>, 18 mM NH<sub>4</sub>Cl, 41 μM nitri-  
167 lo-triacetic acid, 2 mM MgSO<sub>4</sub>, 0.45 mM CaCl<sub>2</sub>, 3 μM FeCl<sub>3</sub>,  
168 1 μM MnCl<sub>2</sub>, 1 μM ZnCl<sub>2</sub>, 0.3 μM (CrCl<sub>3</sub>, H<sub>3</sub>BO<sub>3</sub>, CoCl<sub>2</sub>,  
169 CuCl<sub>2</sub>, NiCl<sub>2</sub>, Na<sub>2</sub>MoO<sub>4</sub>, Na<sub>2</sub>SeO<sub>3</sub>)] supplemented with  
170 20 mM (or 5 mM for protocatechuate) of the desired carbon  
171 source.

### 172 2.3 Metabolome preparation

#### 173 2.3.1 Analytical scale

174 Cells were grown in 5 ml at 30 °C. Metabolite extraction  
175 was adapted from the Metabolomics Service Protocols  
176 from the University of Glasgow (<http://www.polyomics.gla.ac.uk/assets/downloads/MSMetabolomicsPrepCells-Aug2013.pdf>). A saturated overnight culture was diluted in  
177 a fresh medium at an OD<sub>600</sub> = 0.05. 5 ml were transferred in  
178 a well of a 24 deep-well plate (Whatman; reference 7701-  
179 5110). The cells were further grown to an OD<sub>600</sub> between  
180 0.6 and 0.8 in a shaking incubator (Climo Shaker ISF1-X  
181 Kühner). The plate was then centrifuged at 2700×g at 4 °C  
182 for 10 min and the supernatant removed. The cell pellet  
183 was resuspended in 200 μl of water/methanol/acetonitrile  
184 (1:3:1 ratio) and placed in a cold bath (−80 °C) composed  
185 of dry ice and ethanol. After cell freezing, the mixture was  
186 let at 25 °C to complete unfreezing of the cells. This proce-  
187 dure was repeated twice to completely break the cells. The  
188 metabolites were next rocked on a shaker for 1 h at 4 °C. The  
189 metabolites were centrifuged at 5000×g at 4 °C for 10 min.

The supernatant was dried and stored at −80 °C. Before  
LC/MS analysis, the metabolites were suspended with 20 μl  
water and 42 μl 80% acetonitrile and 20% 10 mM ammo-  
nium carbonate (pH 9.9), centrifuged at 5000×g at 4 °C  
for 10 min. The supernatant was finally filtered on 0.22 μm  
(PTFE, Acroprep Advance, Pall).

#### 2.3.2 Preparative scale

For purification of metabolite of *m/z* 211 (M<sub>211</sub>), a satu-  
rated overnight culture was diluted in a fresh medium at  
an OD<sub>600</sub> = 0.05. 5 ml were distributed in each well of a  
24 deep-well plate. Four plates were prepared per day. The  
cells were further grown to an OD<sub>600</sub> between 0.6 and 0.8 in  
a shaking incubator. The four plates were then centrifuged  
at 2700×g at 4 °C for 10 min and the supernatant removed.  
Cell pellets were resuspended in 200 μl of water/methanol/  
acetonitrile (1:3:1 ratio). The plates were placed in a cold  
bath (−80 °C) composed of dry ice and ethanol. After cell  
freezing, the plates were let at 25 °C to complete unfreezing  
of the cells. This procedure was repeated twice to completely  
break the cells. The plates were next rocked on a shaker for  
1 h at 4 °C. The extracted metabolites were pooled in a 50 ml  
Falcon tube and lyophilized and stored at −80 °C. All this  
procedure was repeated three times, for a total of twelve  
24 deep-well plates processed (1.5 l of cell culture). The  
metabolome was resuspended in 7 ml 80% acetonitrile and  
20% 10 mM ammonium acetate (pH 6.8) before purification.

### 2.4 Metabolome derivatization

1,3-Diaminopropane (DAP) was labelled with benzoyl chlo-  
ride for improving LC/MS detection (Aflaki et al. 2014).  
Dried metabolomes from 5 ml cultures were resuspended  
in 250 μl water and basified with 0.5 μl 2M NaOH. 250 μl  
of 4% benzoyl chloride in acetonitrile were added. After  
15 min, the mixture was filtered on 0.22 μm (PTFE, Acro-  
prep Advance, Pall) and injected for LC/MS analysis.

### 2.5 Analytical chromatography

Analyses were conducted using a Dionex Ultimate 3000  
Rapid Separation LC (Thermo Fisher Scientific).

Chromatographic Method 1 used a ZIC®-pHILIC column  
(150 × 4.6 mm<sup>2</sup>; 5 μm; Merck) and was previously reported  
(Stuani et al. 2014).

Chromatographic Method 2 was used for hydrogen/deu-  
terium exchange (HDX) experiments, with deuterated (D<sub>2</sub>O)  
mobile phase. Elution was carried out on a ZIC®-pHILIC  
column (100 × 2.1 mm<sup>2</sup>; 5 μm; Merck) to minimize the use  
of heavy water. Column temperature was set to 15 °C using  
a mobile phase gradient with a flow rate of 0.2 ml/min.  
Mobile phase A consisted of 10 mM ammonium carbonate

in deuterated water and mobile phase B of acetonitrile. The gradient started at 80% B for 1 min, followed by a linear gradient to 40% B at 8 min and remained 4 min at 40% B. The system returned to the initial solvent composition in 3 min and re-equilibrated under these conditions for 15 min. 2.5  $\mu$ l were injected. All experiments done on labelled samples with these new settings were replicated on light samples with the same chromatographic column for comparison.

Chromatographic Method 3 used a Synchronis HILIC column (50  $\times$  2.1 mm<sup>2</sup>; 1.7  $\mu$ m; Thermo Fischer Scientific) and was conducted at 30 °C with a mobile phase gradient at a flow rate of 0.3 ml/min. A consisted of 10 mM ammonium acetate (pH 6.8) and B of acetonitrile. The gradient started at 80% B for 0.3 min, followed by a linear gradient to 40% B at 1.8 min and remained 1.5 min at 40% B. The system returned to the initial solvent composition in 0.5 min and re-equilibrated under these conditions for 3.70 min. 2  $\mu$ l were injected.

Chromatographic Method 4 used a ZIC®-pHILIC column (150  $\times$  2.1 mm<sup>2</sup>; 5  $\mu$ m; Merck) with a mobile phase gradient at a flow rate of 0.2 ml/min at 40 °C. A consisted of 10 mM ammonium carbonate with pH adjusted to 9.9 with NH<sub>4</sub>OH and B of acetonitrile. The gradient started at 80% B for 2 min, followed by a linear gradient to 40% B at 20 min and remained 3 min at 40% B. The system returned to the initial solvent composition in 2 min and re-equilibrated under these conditions for 12.2 min. 5  $\mu$ l were injected.

Chromatographic Method 5 used a ZIC®-pHILIC (50  $\times$  2.1 mm<sup>2</sup>; 5  $\mu$ m; Merck) with a mobile phase gradient at a flow rate of 0.2 ml/min at 40 °C. A consisted of 10 mM ammonium carbonate with pH adjusted to 9.9 with NH<sub>4</sub>OH and B of acetonitrile. The gradient started at 80% B for 0.5 min, followed by a linear gradient to 40% B at 6 min and remained 1.5 min at 40% B. The system returned to the initial solvent composition in 1.5 min and re-equilibrated under these conditions for 4.3 min. 2  $\mu$ l were injected.

Chromatographic Method 6 used an Acquity UPLC BEH C18 column (100  $\times$  2.1 mm<sup>2</sup>; 1.7  $\mu$ m; Waters) and was conducted at 35 °C with a mobile phase gradient at a flow rate of 0.3 ml/min. Mobile phase A consisted of H<sub>2</sub>O and mobile phase B consisted of methanol. The gradient started at 10% B for 1 min, followed by a linear gradient to 70% B at 19 min and remained 5 min at 70% B. The system returned to the initial solvent composition in 5 min and re-equilibrated under these conditions for 10 min. 5  $\mu$ l were injected. For all chromatographic analysis, the autosampler was kept at 4 °C.

## 2.6 Metabolite purification

Metabolite purification was performed on a semi-preparative HPLC system Prominence LC-20AP (Shimadzu, Kyoto, Japan) fitted with a fraction collector FRC-10A (Shimadzu, Kyoto, Japan). The extracted metabolome was first dissolved

and sonicated for 10 min at 4 °C in 6 ml 80% acetonitrile and 20% 10 mM ammonium acetate (pH 6.8). The sample was centrifuged at 4000 $\times$ g for 10 min at 4 °C and the supernatant filtered on 0.22  $\mu$ m (Millipore Millex-GV 13 mm). The filter was further washed with 1 ml of the same solution. The first purification step was conducted using a ZIC®-HILIC column (250  $\times$  10 mm<sup>2</sup>; 5  $\mu$ m; Merck). A mobile phase gradient was used with a flow rate of 4.6 ml/min. Mobile phase A consisted of 10 mM ammonium acetate (pH 6.8) and mobile phase B consisted of acetonitrile. The gradient started at 80% B for 2 min, followed by a linear gradient to 40% B at 22 min and remained 10 min at 40% B. The system returned to the initial solvent composition in 20 min and re-equilibrated under these conditions for 20 min. 200  $\mu$ l were injected (33 injections of 200  $\mu$ l were performed). The compound was monitored at 223 nm and collected in 2.3 ml fractions. Due to the weak UV signal of M211, the eluted fractions were analyzed for the presence of m M211 by LC/MS using Chromatographic Method 3. The fractions of interest were pooled and dried, yielding 1.1 mg of a yellow/pale brown solid residue. The partially purified compound was dissolved in 2 ml 72% acetonitrile and 28% 10 mM ammonium acetate (pH 6.8) and centrifuged at 4000 $\times$ g for 10 min at 4 °C and the supernatant filtered on 0.22  $\mu$ m (Millipore Millex-GV 13 mm). The filter was further washed with 1 ml of the same solution. The second purification step was conducted using the same ZIC®-HILIC column (250  $\times$  10 mm<sup>2</sup>; 5  $\mu$ m; Merck) with an isocratic separation (mobile phase: 72% acetonitrile and 28% 10 mM ammonium acetate, pH 6.8) at a flow rate of 4.6 ml/min. 200  $\mu$ l were injected (13 injections of 200  $\mu$ l were performed). The eluted 2.3 ml fractions were analyzed for the presence of M211 by LC/MS using Chromatographic Method 3. 100  $\mu$ g of pure M211 were obtained as a pale yellow solid matter.

## 2.7 HRMS analyses

High-resolution measurements were obtained with a Velos Pro Orbitrap Elite mass spectrometer (Thermo Fisher Scientific) fitted with a heated electrospray ionization source (HESI) operating in positive and negative ionization modes. In the positive ion mode, the ion spray (IS) was set to +3.5 kV and the capillary temperature at 275 °C. Sheath gas and auxiliary gas flow rates were set at 60% arbitrary units (a.u.) and 44 a.u., respectively. The S-lens RF level was set to 55%. In the negative ion mode, the IS was set to -4.0 kV and the S-lens RF level to 60. Mass spectra were acquired over an  $m/z$  range from  $m/z$  50 up to  $m/z$  1000 with the mass resolution set to 60,000 FWHM at  $m/z$  400. LC/MS data were acquired in raw files and processed with the Qualbrowser module of Xcalibur 2.2 (Thermo Fisher Scientific) to access to elemental compositions. Fragmentation experiments were performed under collision induced dissociation

(CID) and higher energy dissociation (HCD) conditions. For CID and HCD, normalized collision energies (NCE) of 22% and 28% in positive mode and 33% and 75% in negative mode, respectively were applied.

## 2.8 NMR analyses

Samples were dissolved in D<sub>2</sub>O:H<sub>2</sub>O (10:90). NMR experiments were performed on a Bruker Advance 600-MHz NMR spectrometer equipped with a 1.7 mm cryogenic probe.

The <sup>1</sup>H NMR water signal from the polar fraction was suppressed by means of excitation sculpting (Bruker ZGESGP pulse program). Additional <sup>13</sup>C NMR spectra were acquired for each sample. <sup>1</sup>H-<sup>1</sup>H COSY, <sup>1</sup>H-<sup>13</sup>C HSQC, <sup>1</sup>H-<sup>13</sup>C HMBC and <sup>1</sup>H-<sup>15</sup>N HMBC experiments was only carried out for the purified metabolite sample.

Chemical shifts (expressed in ppm) of <sup>1</sup>H NMR spectra were referenced to the solvent peaks δ H 4.79 for D<sub>2</sub>O.

3-((3-Aminopropyl)amino)-4-hydroxybenzoic acid (M211; APAH):

<sup>1</sup>H NMR (H<sub>2</sub>O/D<sub>2</sub>O (90:10), 600 MHz): 7.22 (1H, d, *J*=2.0 Hz, H<sub>2</sub>), 7.20 (1H, dd, *J*=8.5 and 2.0 Hz, H<sub>6</sub>), 6.77 (1H, d, *J*=8.5 Hz, H<sub>5</sub>), 3.20 (2H, t, *J*=7.4 Hz, H<sub>1</sub>'), 3.03 (2H, t, *J*=7.4 Hz, H<sub>3</sub>'), 1.92 (2H, quint, *J*=7.4 Hz, H<sub>2</sub>'); <sup>13</sup>C NMR (H<sub>2</sub>O/D<sub>2</sub>O (90:10), 150 MHz): 176.0 (C<sub>1</sub>'), 148.5 (C<sub>4</sub>), 136.2 (C<sub>3</sub>), 128.6 (C<sub>1</sub>), 121.7 (C<sub>6</sub>), 114.5 (C<sub>5</sub>), 114.5 (C<sub>2</sub>), 41.6 (C<sub>1</sub>'), 38.4 (C<sub>3</sub>'), 26.8 (C<sub>2</sub>').

5-((3-Aminopropyl)amino)-2-hydroxybenzoic acid (SN0079):

<sup>1</sup>H NMR (D<sub>2</sub>O, 600 MHz): 7.25 (1H, d, *J*=2.9 Hz), 6.96 (1H, dd, *J*=8.7 and 2.9 Hz), 6.84 (1H, d, *J*=8.7 Hz), 3.16 (2H, t, *J*=7.1 Hz), 3.09 (2H, t, *J*=7.6 Hz), 1.94 (2H, quint, *J*=7.4 Hz); <sup>13</sup>C NMR (D<sub>2</sub>O, 150 MHz): 176.0, 153.8, 140.5, 123.0, 118.9, 117.6, 116.7, 43.0, 38.3, 26.9.

4-((3-Aminopropyl)amino)-2-hydroxybenzoic acid (SN0080):

<sup>1</sup>H NMR (D<sub>2</sub>O, 600 MHz): 7.51 (1H, d, *J*=8.6 Hz), 6.2 (1H, dd, *J*=8.6 and 2.1 Hz), 6.07 (1H, d, *J*=2.1 Hz), 3.13 (2H, t, *J*=6.7 Hz), 2.96 (2H, t, *J*=7.7 Hz), 1.85 (2H, quint, *J*=7.3 Hz); <sup>13</sup>C NMR (D<sub>2</sub>O, 150 MHz): 176.0, 161.6, 153.3, 131.9, 107.6, 105.7, 98.3, 40.0, 37.5, 26.5.

2-((3-Aminopropyl)amino)-5-hydroxybenzoic acid (SN0123):

<sup>1</sup>H NMR (D<sub>2</sub>O, 600 MHz): 7.29 (1H, d, *J*=3.0 Hz), 6.96 (1H, dd, *J*=8.8 and 3.0 Hz), 6.86 (1H, d, *J*=8.8 Hz), 3.25 (2H, t, *J*=6.8 Hz), 3.10 (2H, t, *J*=7.6 Hz), 1.97 (2H, quint, *J*=7.2 Hz). <sup>13</sup>C NMR (D<sub>2</sub>O, 150 MHz): 175.3, 147.1, 142.3, 123.0, 119.7, 117.2, 116.0, 41.7, 37.6, 26.3.

4-((3-Aminopropyl)amino)-3-hydroxybenzoic acid (SN0124):

<sup>1</sup>H NMR (D<sub>2</sub>O, 600 MHz): 7.44 (1H, dd, *J*=8.2 and 1.5 Hz), 7.34 (1H, d, *J*=1.6 Hz), 6.79 (1H, d, *J*=8.2 Hz),

3.33 (2H, t, *J*=6.8 Hz), 3.12 (2H, t, *J*=7.5 Hz), 2.00 (2H, quint, *J*=7.2 Hz). <sup>13</sup>C NMR (D<sub>2</sub>O, 150 MHz): 175.5, 143.0, 139.8, 125.3, 122.9, 115.1, 110.7, 40.2, 37.6, 26.2.

## 2.9 APAH quantification

A calibration line for APAH (3-((3-aminopropyl)amino)-4-hydroxybenzoic acid) was required to calculate its in vivo concentration. The calibration line was obtained using calibration solutions containing 0, 1, 2, 5, 10 and 19 μM of synthetic APAH spiked in metabolomes from succinate-grown cells (devoid of APAH), to take into account the matrix effect. These spiked metabolomes were analyzed on our Velos Pro Orbitrap Elite in the positive mode using Chromatographic Method 4. The peak areas from extracted ion chromatograms of APAH were integrated and the values used to build the calibration line. Next, to estimate APAH concentration in the cell, metabolomes from 13 independent 5 ml cultures of quinate-grown cells (OD<sub>600</sub>=0.47±0.02) were used. Cell cultures (succinate and quinate) and metabolome preparation were conducted as described above. The lyophilized metabolomes were resuspended with 20 μl water and 42 μl 80% acetonitrile and 20% 10 mM ammonium carbonate (pH 9.9). Samples were filtered on 0.22 μm prior to injection.

## 3 Results and discussion

### 3.1 LC/HRMS/MS<sup>n</sup> analysis of an unknown metabolite of *m/z* 211

Among the compounds exclusively formed in quinate-grown cells, we considered here an ion that, analyzed with LC-HRMS, has a long retention time (14.3 min) on the hydrophilic zwitterionic ZIC@-pHILIC column (Chromatographic Method 1, see "Material and methods" section) and led to intense ionization signal in the positive mode at *m/z* 211.1074 (Fig. 1a, b). The compound was also detected in the negative mode at *m/z* 209.0934. These two *m/z* values were anticipated to be the protonated [M+H]<sup>+</sup> and deprotonated form [M-H]<sup>-</sup> of the same molecule, respectively. The monoisotopic mass of the protonated form of this unknown metabolite, which we called M211 (metabolite of *m/z* 211), was consistent with an elemental composition of C<sub>10</sub>H<sub>15</sub>O<sub>3</sub>N<sub>2</sub><sup>+</sup> (-1.6 ppm off the theoretical mass) and with its first natural isotope abundance (M+1 = 11.1%; Fig. 1b). Elemental composition was validated by applying the Seven Golden Rules (Kind and Fiehn 2007). The long retention time of M211, associated with detection in both ionization modes suggest a very polar structure carrying acidic and basic functional groups. Photodiode array (PDA) detection indicated UV absorption (Fig. 1c) with maxima at 224, 259,

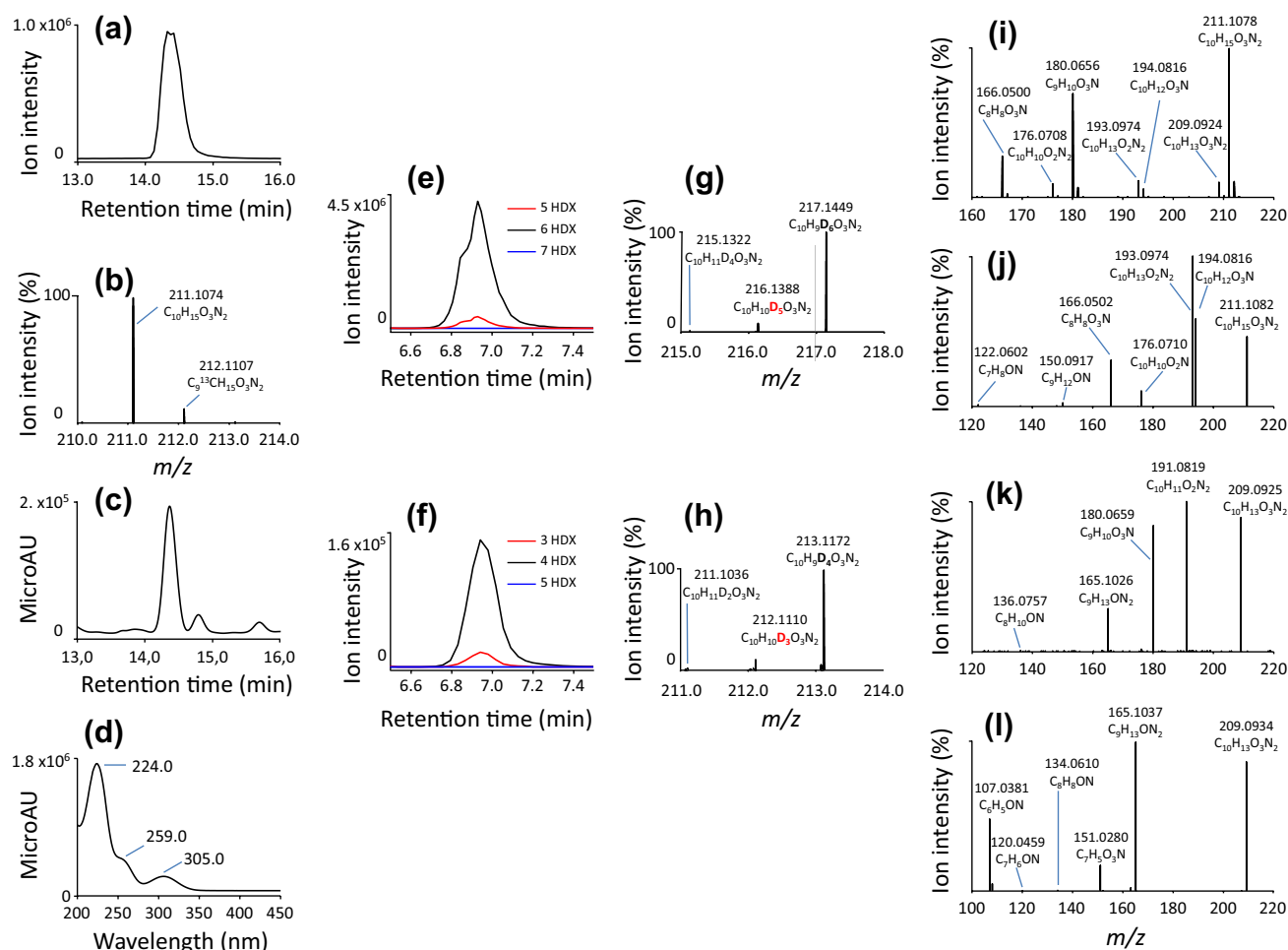


**Fig. 1** LC/MS analysis of M211 in the metabolome of *Acinetobacter baylyi* ADP1. **a** EIC corresponds to the protonated metabolite molecule  $[M+H]^+$  at  $m/z$  211.1077 in a metabolome from ADP1 quinate-grown cells (5 ppm accuracy). **b** Zoom on the mass spectrum of M211 (close up) in the positive mode. **c** LC/PDA chromatogram of M211. **d** UV-visible spectrum of M211. **e** EICs of deuterated species of M211 after HDX in the positive ionization mode at  $m/z$  216.1391 (red line), 217.1454 (black line) and 218.1487 (blue line) at 5 ppm accuracy. **f** EICs of deuterated species of M211 after HDX in the

negative ionization mode at  $m/z$  212.1120 (red line), 213.1187 (black line) and 214.1246 (blue line) at 5 ppm accuracy. **g** Zoom on the mass spectrum of the deuterated forms of M211 in the positive ionization mode. **h** Zoom on the mass spectrum of the deuterated forms of M211 in the negative ionization mode. **i** HRMS of M211 in the positive ionization mode. **j** HCD spectrum of M211 in the positive ionization mode (28% NCE). **k** HCD spectrum of the oxidized form of M211 in the positive ionization mode ( $m/z$  209.0921) at 28% NCE. **l** HCD spectrum of M211 in the negative mode ( $m/z$  209.0932) at 75% NCE

438 and 302 nm (Fig. 1d) that are evocative of an aromatic moiety (Singh et al. 2007).

439  
440 Accurate mass and elemental composition of M211  
441 matched to only two compounds present in Metlin and  
442 KEGG databases: aprobarbital and 2,6-dihydropseudoni-  
443 cotine. These molecules harbor 2 and 3 mobile protons,  
444 respectively (Fig. S1). To check whether these molecules  
445 could correspond to M211, we determined its mobile pro-  
446 ton number. This was established in positive and negative  
447 ionization modes using in-solution hydrogen/deuterium  
448 exchange (HDX) approach (Chromatographic Method 2).  
449 Six mobile protons were observed in the positive mode  
450 and four in the negative mode; i.e. five mobile protons  
451 for the neutral form of the molecule (Fig. 1e–h). This

result invalidated the structures proposed by the databases  
and confirmed that M211 was a previously unreported  
metabolite.

452  
453  
454  
455 Mass spectra recorded in the positive mode displayed  
456 M211 and a series of other ions with the same extracted  
457 ion chromatogram (EIC) shape: a major ion at  $m/z$  180 and  
458 minor ones at  $m/z$  166, 176, 193, 194 and 209 (Fig. 1i).  
459 This latter probably originated from in-source oxidation of M211.  
460 The similar chromatographic shape of these ions suggests  
461 they could be generated by in-source dissociation of the pre-  
462 cursor ion at  $m/z$  211 (Fig. S2a).

463  
464  
465 In the negative mode M211 was detected at  $m/z$  209.  
Two others weakly abundant ions at  $m/z$  165 and  $m/z$   
107 observed in the mass spectrum displayed similar

466 chromatographic shapes, and originated from in-source  
467 dissociation of  $m/z$  209.

468 Fragmentation spectra were recorded under collision  
469 induced dissociation (CID) and higher energy dissociation  
470 (HCD) conditions. Under HCD, small size fragment ions  
471 become significantly more abundant. In the positive mode  
472 (Fig. 1j), fragmentation spectra display two main product  
473 ions: a major one at  $m/z$  193 (water loss) and a slightly less  
474 abundant one at  $m/z$  194 ( $\text{NH}_3$  loss). Less abundant  $m/z$   
475 176 and  $m/z$  166 product ions are related to the consecutive  
476 losses of  $[\text{NH}_3 + \text{H}_2\text{O}]$  and the release of  $[\text{C}_2\text{H}_7\text{N}]$ , respec-  
477 tively. The neutral  $[\text{C}_2\text{H}_7\text{N}]$  moiety formally corresponds  
478 to saturated alkyl amine. The  $m/z$  166 product ion was also  
479 formed during consecutive fragmentation of the  $m/z$  194  
480 precursor (sequential  $\text{MS}^3$  experiments), as illustrated in  
481 Fig. S2b. This ion is related to the loss of  $\text{C}_2\text{H}_4$  from  $m/z$   
482 194 ion produced by the loss of ammonium from  $m/z$  211  
483 precursor ion. Therefore,  $[\text{C}_2\text{H}_7\text{N}]$  probably corresponds  
484 to ethylamine rather than dimethylamine. HCD fragmenta-  
485 tion also yielded very weak signals at  $m/z$  150 and  $m/z$  122,  
486 which likely originated from consecutive fragmentation  
487 of  $m/z$  194 by the loss of  $\text{CO}_2$  and  $[\text{CO}_2 + \text{C}_2\text{H}_4]$ , respec-  
488 tively. These ions were also observed in the sequential  
489  $\text{MS}^3$  experiments of the selected  $m/z$  194 (Fig. S2b). All  
490 these fragment ions were present in the mass spectrum,  
491 too. Ion  $m/z$  180 was not detected in the fragmentation  
492 spectrum of M211, using either CID or HCD. However,  
493 it was very abundant in the fragmentation spectrum of its  
494 oxidized form at  $m/z$  209 (Fig. 1k), indicating that  $m/z$  180  
495 observed in the mass spectrum of M211 originated mainly  
496 from in-source dissociation of  $m/z$  209. In addition, the  
497 number of mobile protons observed on the one side for  
498 M211 (5 for the neutral species) and on the other side for  
499  $m/z$  209 (3 for the neutral form) and  $m/z$  180 (mostly 2 and  
500 in a much lesser extent 3 for the neutral form) are in agree-  
501 ment with the loss of  $\text{CH}_2\text{NH}$  (1 mobile proton) from  $m/z$   
502 209 rather than the release of  $\text{CH}_3\text{NH}_2$  (2 mobile protons)  
503 from M211 (Fig. S2c-f).

504 In the negative mode, HCD spectra of the selected ion  
505  $m/z$  209 yielded a main product ion at  $m/z$  165 ( $\text{CO}_2$  loss)  
506 along with two less abundant radical ions at  $m/z$  107 and  $m/z$   
507 151 (Fig. 1l). These latter were formed after the loss of the  
508 radical ion  $\text{C}_3\text{H}_8\text{N}^\cdot$ , either from  $m/z$  165 (consecutive loss,  
509 which is also observed in  $\text{MS}^3$  experiments on the selected  
510 precursor  $m/z$  165 ion) or from  $m/z$  209, respectively.

511 The following assumptions can be made from the frag-  
512 mentation spectra: in the negative mode, a major loss of  
513  $\text{CO}_2$  is characteristic of the presence of a carboxylic group.  
514 In addition, the formation of an odd electron product ion  
515 such as  $m/z$  107  $[\text{C}_6\text{H}_5\text{ON}]^\cdot$  with a degree of unsatura-  
516 tion of 5 (5.5 for the parent ion  $m/z$  209) together with UV  
517 data (Fig. 1a, b) suggests the presence of an aromatic core.  
518 According to its elemental composition, this relatively stable

radical anion should represent a phenol derivative (Afonso  
et al. 2010).

Generally, an abundant loss of  $\text{NH}_3$  in the positive mode  
is due to the presence of a primary aliphatic amino group.  
Here, a single ammonium loss suggests the presence of a  
single primary aliphatic amine in the unknown structure  
(Levsen et al. 2007). Therefore, taking into account the total  
number of mobile protons (five for the neutral species), a  
structure that involves N-containing heterocycle should be  
excluded. A loss of  $\text{H}_2\text{O}$  in the positive mode can be related  
to the presence of either a carboxylic group or an aliphatic  
OH group (Levsen et al. 2007). Considering on the one hand  
a single water loss, the presence of one carboxylic group  
(two O-atoms), and on the other hand a total number of three  
oxygen atoms and the previously discussed existence of an  
aromatic (phenol) core, we anticipate a phenolic group rather  
than an aliphatic hydroxyl group. Thus, taking into account  
five mobile protons for the uncharged molecule, one for the  
carboxylic group, two for the primary amino group and one  
for the phenolic hydroxyl group, the molecule should involve  
a secondary amino group with one more mobile proton.

In conclusion, LC-HRMS/ $\text{MS}^n$  data suggest that the  
unknown metabolite contains an aromatic moiety, possi-  
bly a phenol ring, a carboxylic group along with primary  
and secondary amines, but de novo interpretation of mass  
spectrometry data did not allow to completely elucidate its  
chemical structure.

### 3.2 NMR analysis of purified M211

NMR was considered to achieve the complete struc-  
tural elucidation of M211. The metabolite was purified  
from 1.5 l of bacterial culture in MA medium containing  
20 mM quinate as the carbon source. Purification was  
carried out using HILIC-phase chromatography and led  
to 100  $\mu\text{g}$  of a pale yellow solid (see “Material and meth-  
ods” section). Extensive 1D- and 2D-NMR analyses ( $^1\text{H}$ ,  
 $^{13}\text{C}$ ,  $^1\text{H}$ - $^1\text{H}$ -COSY,  $^1\text{H}$ - $^{13}\text{C}$ -HSQC,  $^1\text{H}$ - $^{13}\text{C}$ -HMBC and  
 $^1\text{H}$ - $^{15}\text{N}$ -HMBC) were performed (see Table 1 and Data-  
set\_S1). The  $^1\text{H}$ -NMR spectrum clearly confirmed the  
presence of an aromatic ring bearing three protons. Their  
multiplicity (Table 1; Fig. 2a) indicated a 1,2,4-trisubsti-  
tution pattern (Fig. 2b). The set of three aliphatic signals,  
integrating each for two protons, suggested a propylene  
moiety further confirmed by several cross-correlations  
peaks visible in COSY spectrum (Fig. 2c, d). Combining  
 $^1\text{H}$  and  $^{13}\text{C}$  chemical shifts of aliphatic signals allowed  
us to conclude to a 1,3-diaminopropyl substructure, in  
agreement with HRMS/ $\text{MS}^n$  conclusions that predicted  
the presence of primary and secondary amines (Fig. 2d).  
Cross correlation peak between proton  $\text{H}_1$  and carbon  
 $\text{C}_3$  in HMBC spectrum (Fig. 2e) unambiguously demon-  
strated that the secondary amine is responsible for the



**Table 1**  $^1\text{H}$ - and  $^{13}\text{C}$ -NMR spectral data of  $m/z$  211 [600/150 MHz,  $\text{H}_2\text{O}/\text{D}_2\text{O}$  90:10,  $\delta$  (ppm), J (Hz)]

Proton	Chemical shifts $\delta_{\text{H}}$	integration	multiplicity	Coupling constants (Hz)	COSY signals	$^1\text{H}$ - $^{13}\text{C}$ (HSQC, $^1\text{J}$ )	$^1\text{H}$ - $^{13}\text{C}$ (HMBC, $^3\text{J}, ^4\text{J}$ )	$^1\text{H}$ - $^{15}\text{N}$ (HMBC, $^3\text{J}, ^4\text{J}$ )
1	–	–	–	–	–	128.6	–	–
2	7.22	1	d	1.95	H6	114.5	C6 C4 C1''	$\text{N}_\alpha$
3	–	–	–	–	–	136.2	–	–
4	–	–	–	–	–	148.5	–	–
5	6.77	1	d	8.50	H6	114.5	C1 C3 C4	$\text{N}_\alpha$
6	7.20	1	dd	8.50 1.95	H5 H2	121.7	C2 or C5 C4 C1''	–
1'	3.20	2	t	7.40	H2'	41.6	C3' C2' C3	–
2'	1.92	3	q	7.40 7.40	H1' H3'	26.8	C1' C3'	$\text{N}_\alpha$ $\text{N}_\beta$
3'	3.03	2	t	7.40	H2'	38.4	C1' C2'	–
1''	–	–	–	–	–	176	–	–

linkage of the aliphatic moiety to the aromatic ring. Characteristic chemical shift values of 147 and 176 ppm for carbon  $\text{C}_4$  and  $\text{C}_{1''}$  confirmed the presence of phenolic and carboxylic moieties (see Table 1 and Dataset S1). HMBC experiments indicated that the carboxylic function is indeed branched onto the aromatic system (Fig. 2f). Expected labile protons for amine, phenol and carboxylic acid groups could not be observed in  $^1\text{H}$  NMR neither in organic solvents (dimethylformamide- $d_6$ , acetonitrile- $d_3$ ) nor in aqueous solutions (90/10  $\text{H}_2\text{O}/\text{D}_2\text{O}$  and 90/10  $\text{H}_2\text{O}/\text{D}_2\text{O}$  + 1% trifluoroacetic acid). Another difficulty arose from the superposition of two signals in  $^{13}\text{C}$  NMR spectrum at 114.5 ppm (Fig. 2g). Finally, we investigated the relative position of aromatic substituents using  $^1\text{H}$ - $^{13}\text{C}$ -HMBC and  $^1\text{H}$ - $^{15}\text{N}$ -HMBC experiments. Unfortunately, observed long-ranged  $^1\text{H}$ - $^{13}\text{C}$  and  $^1\text{H}$ - $^{15}\text{N}$  correlations (Fig. 2f, h) did not allow us to draw any firm conclusion. Indeed,  $^2\text{J}(^1\text{H}-^{13}\text{C})$ ,  $^3\text{J}(^1\text{H}-^{13}\text{C})$  and  $^4\text{J}(^1\text{H}-^{13}\text{C})$  on the one side and  $^2\text{J}(^1\text{H}-^{15}\text{N})$ ,  $^3\text{J}(^1\text{H}-^{15}\text{N})$  and  $^4\text{J}(^1\text{H}-^{15}\text{N})$  on the other side are known to lead to coupling values of similar frequency in aromatic systems (Martin and Williams 2008; Martin and Hadden 2000). At that stage, the complete structure elucidation of M211 was still not achieved as six regioisomers remained plausible (Fig. 3).

### 3.3 Structure determination of M211 by comparison to the synthetic standards

To help raising the ambiguity, five out of the six possible compounds were synthesized: 5-((3-aminopropyl)amino)-2-hydroxybenzoic acid (SN0079), 4-((3-aminopropyl)amino)-2-hydroxybenzoic acid (SN0080), 2-((3-aminopropyl)amino)-5-hydroxybenzoic acid (SN0123), 4-((3-aminopropyl)amino)-3-hydroxybenzoic acid (SN0124) and 3-((3-aminopropyl)amino)-4-hydroxybenzoic acid (SN0140).  $^1\text{H}$  and  $^{13}\text{C}$  NMR analyses were then recorded in the same manner as for the purified metabolite (Dataset\_S1). Data clearly showed a very high similarity between M211 and SN0140 in detriment of all other structures. The observed slight  $^1\text{H}$  chemical shift difference between M211 and SN0140 probably originated from the elevated number of protonable functions highly sensitive to pH and/or to concentration due to inter-/intra-Hydrogen bonding (Fig. S3). To confirm the structural assignment, the standards along with a metabolome from ADP1 quinate-grown cells were further analyzed by LC/MS (Chromatographic Method 1). According to comparison of its retention time and  $\text{MS}^2$  spectrum with the reference compounds, M211 was eventually unambiguously identified as 3-((3-aminopropyl)

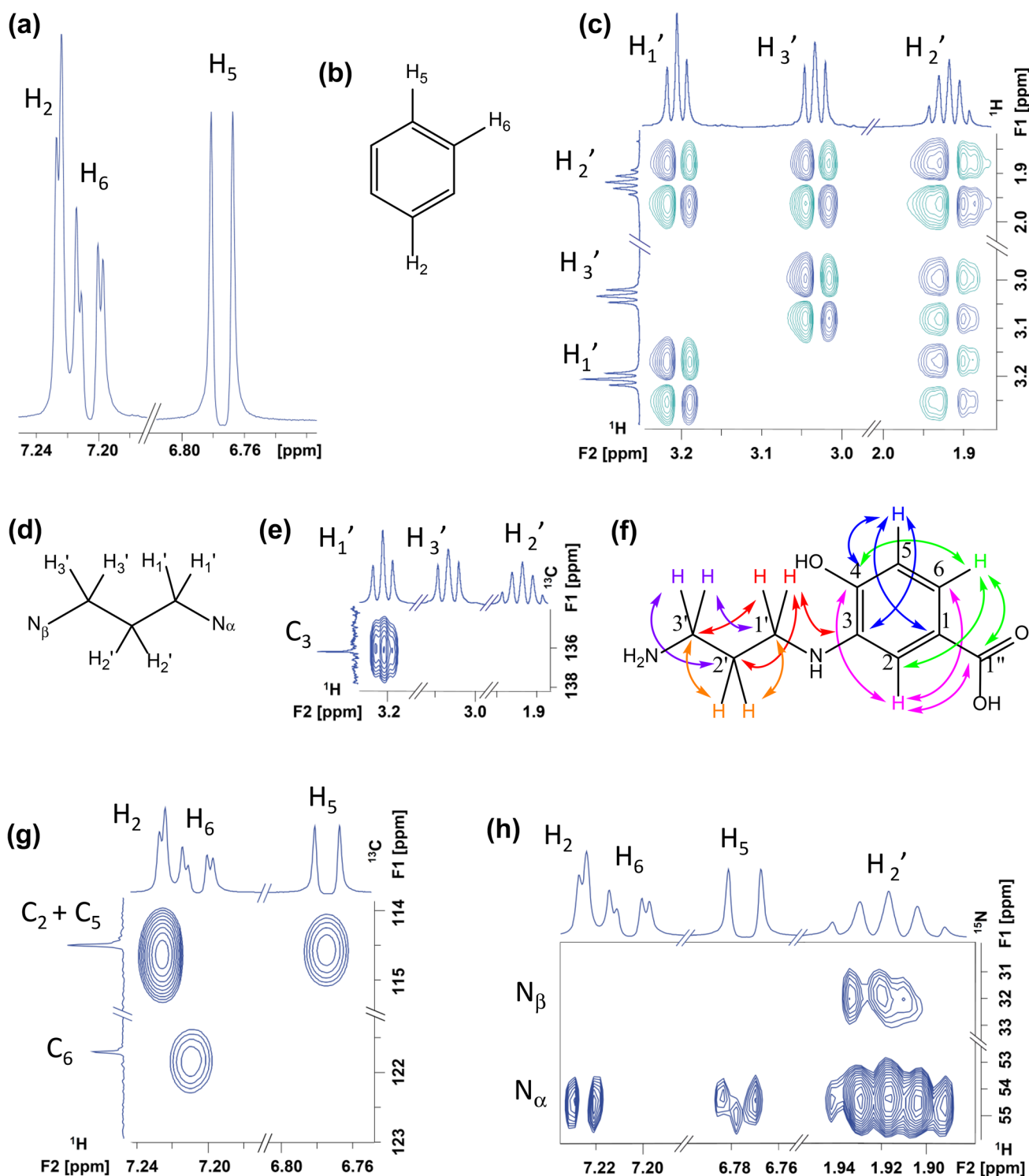
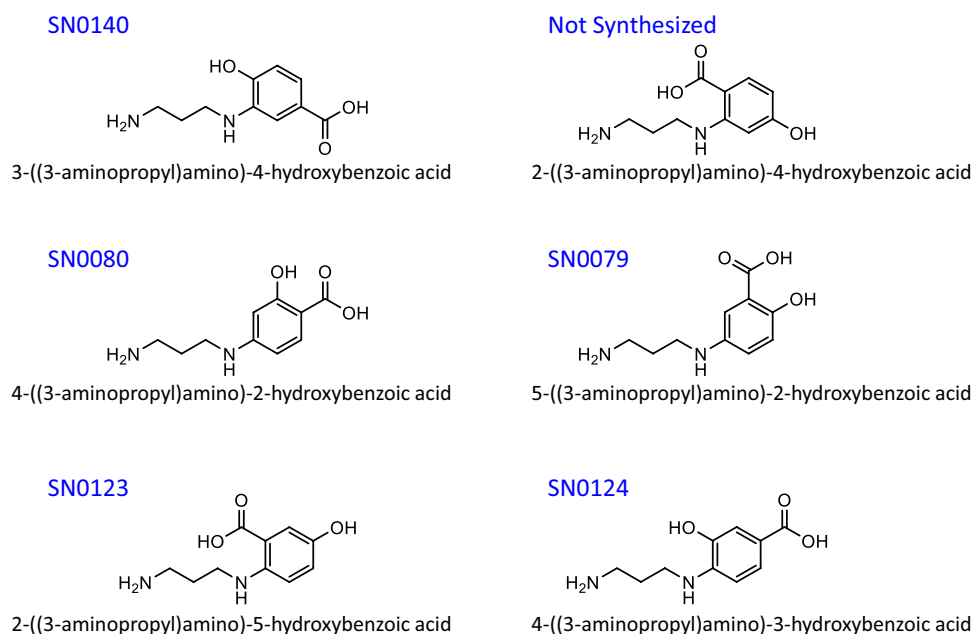


**Fig. 2** NMR analysis of purified M211. **a** Aromatic region of  $^1\text{H}$ -NMR spectrum. **b** Proposed relative positions of aromatic protons based on  $^1\text{H}$ -NMR analysis. **c** Aliphatic region of  $^1\text{H}$ - $^1\text{H}$  COSY spectrum. **d** Proposed 1,3-diaminopropyl side chain based on  $^1\text{H}$ ,  $^{13}\text{C}$  and  $^1\text{H}$ - $^1\text{H}$  COSY NMR analyses. **e** Extract of  $^1\text{H}$ - $^{13}\text{C}$  HMBC NMR

spectrum showing  $\text{C}_3$ - $\text{H}_1'$  correlation. **f**  $^1\text{H}$ - $^{13}\text{C}$  HSQC NMR correlations placed on the proposed M211 structure. **g** Extract of  $^1\text{H}$ - $^{13}\text{C}$  HSQC NMR spectrum showing the superposition of two carbons on  $^{13}\text{C}$ -NMR spectrum. **h** Extract of  $^1\text{H}$ - $^{15}\text{N}$  HMBC NMR spectrum showing all cross correlations between  $^1\text{H}$  and  $^{15}\text{N}$  (natural abundance)

**Fig. 3** Possible structures for M211. Synthesized compounds are indicated by their name of manufacturing



617 amino)-4-hydroxybenzoic acid (APAH), as illustrated in Fig.  
618 S4.

varied in a similar manner sevenfold (Stuani et al. 2014,  
Online Resource 2, Table S-6).

### 3.4 Quantification of APAH in ADP1

619 In vivo quantification of APAH was conducted by  
620 LC–HRMS analysis using synthetic APAH. The calibration  
621 line (Chromatographic Method 4) was obtained by spiking  
622 metabolomes of succinate-grown cells (that are devoid of  
623 APAH) with known amounts of synthetic APAH, to over-  
624 come matrix effects. APAH was quantified according to its  
625 EIC area in metabolomes from independent quinate-grown  
626 cultures (Fig. S5). Assuming the same internal volume 2.3  
627  $10^{-9}$   $\mu$ l for ADP1 as for *E. coli* (Bazile et al. 1992), we  
628 estimated the cellular concentration of APAH to  $7 \pm 4$  mM.  
629 APAH is thus present in ADP1 at a high abundance, which  
630 could affect osmolality. To draw a comparison, in *E. coli*  
631 the concentration of 70% of quantified metabolites is below  
632 the millimolar range (Bennett et al. 2009). Its abundance  
633 should be related to its role in the cell, as low metabolite  
634 concentrations are favorable for avoiding osmotic stress and  
635 disadvantageous spontaneous reactions (Bennett et al. 2009).  
636 Data in Fig. S5 indicated a wide variation of APAH in the  
637 metabolomes (between 2 and 19 mM). This unexplained  
638 variability cannot be attributed to incorrect handling of the  
639 cells during metabolomics sampling. Here, before metabo-  
640 lite extraction, culture centrifugation may have yield a cel-  
641 lular stress that caused the observed variation in APAH  
642 concentrations. However, in our previous study in which  
643 rapid cell quenching was combined with cell inactivation  
644 to ‘freeze’ the microbial metabolism, peak areas of APAH  
645

### 3.5 Hypotheses for APAH biosynthesis

648 APAH is formed in quinate-grown cells but not in succinate  
649 grown-cells (Stuani et al. 2014, Online Resource 2, Table  
650 S-6). Quinate is metabolized through the  $\beta$ -keto adipate  
651 pathway (Young et al. 2005). Most aromatic compounds  
652 are mainly degraded by this pathway through the formation  
653 of catechol (catechol branch) or protocatechuate (protocat-  
654 echuate branch). From catechol and protocatechuate, a paral-  
655 lel but separate branch converts them into succinyl-CoA and  
656 acetyl-CoA which can enter central metabolism through the  
657 TCA cycle (Fig. S6). Quinate is metabolized via the proto-  
658 catechuate branch.

659 From a structural point of view, APAH is evocative  
660 of two metabolites: protocatechuate on the one side and  
661 1,3-diaminopropane (DAP) on the other side. DAP is pre-  
662 sented as the major polyamine in the genus *Acinetobacter*,  
663 with concentrations up to 2.5  $\mu$ mol/g wet cell (Hamana and  
664 Matsuzaki 1992). We hypothesized that APAH may result  
665 from an enzymatic condensation of these two metabolites.  
666 Both protocatechuate and DAP are indeed present in ADP1  
667 quinate-grown cells (Fig. 4). To gain insight in APAH bio-  
668 synthesis, we explored the feasibility of a spontaneous reac-  
669 tion between protocatechuate and DAP. We mixed a 20 mM  
670 aqueous solution of protocatechuate with a 500 mM aque-  
671 ous solution of DAP hydrochloride at a molar ratio of 1:2  
672 (pH 7). After 30 min, we diluted twofold the solution in  
673 80% acetonitrile and 20% 10 mM ammonium carbonate (pH  
674 9.9) before LC/MS analysis (Chromatographic Method 1).  
675

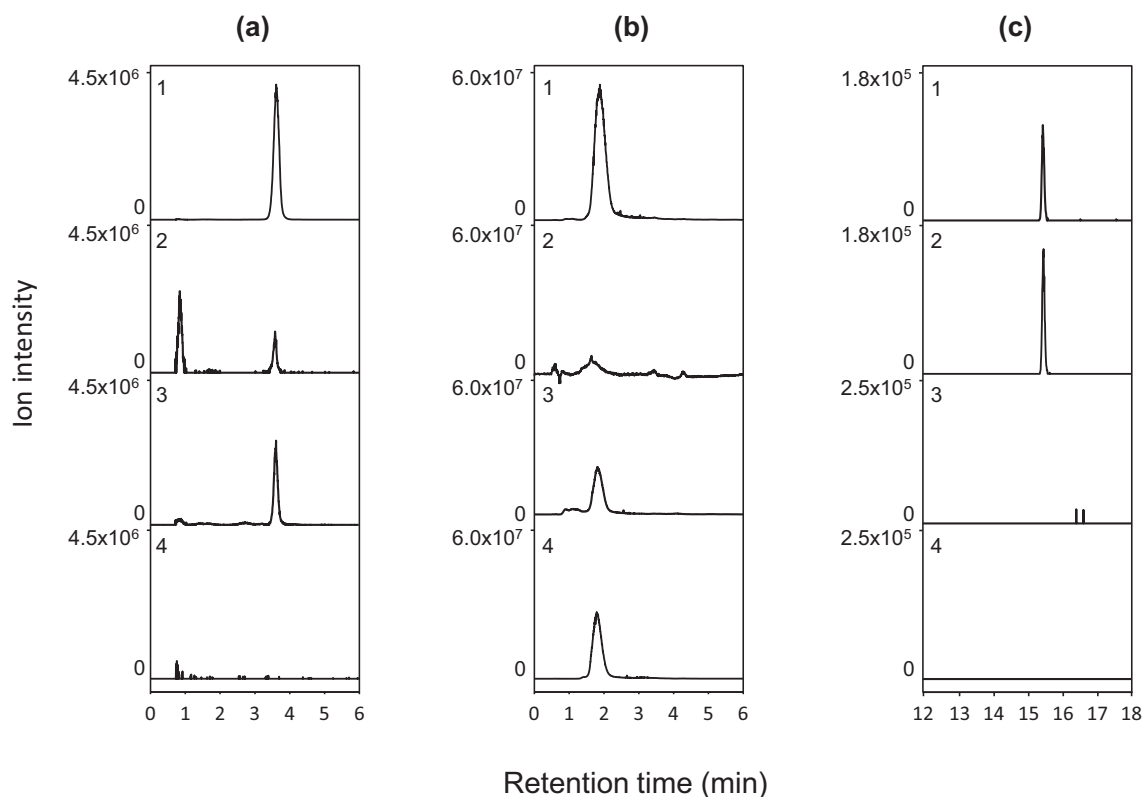


**Fig. 4** Screening of different metabolomes for the presence of M211, protococatechuate and 1,3-diaminopropane. **a** EICs correspond to the  $([M+H]^+)$  of  $m/z$  211.1077 in the positive mode. **b** EICs correspond to the  $([M-H]^-)$  of protococatechuate ( $m/z$  153.0193) in the negative mode. **c** EICs correspond to the  $([M+H]^+)$  of the product of conjugation of 1,3-diaminopropane with two benzoyl groups in the positive

mode ( $m/z$  283.1441). All chromatograms were extracted at 5 ppm accuracy. Metabolomes were prepared from ADP1 quinate-grown cells (1), ADP1 benzyl alcohol-grown cells (2), *P. putida* KT4440 quinate grown cells (3) and *R. eutropha* H16 protococatechuate grown cells (4). Chromatograms in a2, a4 and b2 were magnified 100-fold. Chromatograms in a3, c3 and c4 were magnified tenfold

676 Two peaks of similar intensities were observed at  $m/z$  211  
 677 (positive mode) consistent with the formation of two isom-  
 678 ers. According to their retention times and fragmentation  
 679 patterns, they corresponded to APAH and 4-((3-aminopropyl)amino)-3-hydroxybenzoic acid (SN0124), indicating  
 680 that DAP can react with both hydroxyl groups of protocat-  
 681 echuate (Fig. S7). The reaction yield for APAH was very  
 682 low (0.06%) and its concentration was estimated to be only  
 683 0.3  $\mu$ M. These data thus indicate that the reaction, thermo-  
 684 dynamically feasible, could be enzyme-catalyzed. According  
 685 to this postulate, the formation of APAH should be strictly  
 686 correlated to the presence of both DAP and protococatechuate  
 687 in the cell.  
 688

689 We thus examined whether the presence of APAH was  
 690 restricted to quinate metabolism solely or could be also  
 691 linked to the catechol branch. To this end, we analyzed the  
 692 metabolomes of ADP1 grown on benzyl alcohol, a com-  
 693 pound whose degradation feeds into the catechol branch  
 694 (Fig. S6). Data analysis revealed that APAH is formed in  
 695 these conditions, albeit more weakly than in quinate-grown  
 696 cells (Fig. 4a), but in quantity that can nonetheless be

697 compared to that obtained in protococatechuate-grown cells  
 698 (Fig. S8). However, although DAP was present, protocate-  
 699 chuate was not detected in ADP1 growing on benzyl alcohol  
 700 (Fig. 4b). The weak signal detected in the metabolome of  
 701 benzyl alcohol-grown cells did not match with the reten-  
 702 tion time of protococatechuate and displayed a different  $MS^2$   
 703 spectrum. This suggested that APAH is not formed from  
 704 protococatechuate and indicates that APAH biosynthesis is  
 705 neither restricted to quinate degradation nor to the proto-  
 706 catechuate branch of the  $\beta$ -ketoacid pathway. We next  
 707 wondered about the presence of APAH in other organisms  
 708 harboring the quinate degradation pathway. Genome con-  
 709 text analyses conducted on the MicroScope platform (<https://www.genoscope.cns.fr/agc/microscope/home/index.php>)  
 710 showed that clusters of genes orthologous to *pca* operon  
 711 encoding the enzymes for protococatechuate degradation  
 712 (Siehler et al. 2007) are present in the genome of organ-  
 713 isms such as *Pseudomonas putida* KT4440 and *Rasltionia*  
 714 *eutropha* H16. Despite the absence of genes orthologous  
 715 to *qui* operon in *P. putida* for converting quinate to pro-  
 716 tococatechuate, this organism was nevertheless reported to  
 717

718 grow with quinate as the sole carbon source (Jimenez et al.  
 719 2002). Regarding *R. eutropha* H16, its genome does not har-  
 720 bor the *qui* operon either and cannot grow on quinate. We  
 721 thus analyzed the metabolomes of *P. putida* and *R. eutropha*  
 722 grown on quinate and protocatechuate, respectively, for the  
 723 presence of APAH. We detected APAH in *P. putida* but  
 724 not in *R. eutropha* (Fig. 4a). This result emphasizes that  
 725 APAH is not restricted to ADP1 and is produced at least in  
 726 another  $\gamma$ -proteobacterium. On the other hand, its absence  
 727 in *R. eutropha* eliminates a strict association between its  
 728 synthesis and quinate/protocatechuate catabolism. Moreover,  
 729 DAP was not observed in *P. putida* (Fig. 4c). Together, these  
 730 results suggest that neither protocatechuate nor DAP is a  
 731 biosynthetic precursor of APAH. APAH origin and function  
 732 remain unknown. The metabolite is not excreted (Fig. S9)  
 733 as APAH could not be detected in the medium of a culture  
 734 at OD<sub>600</sub> = 0.8, although APAH synthesis is maximal at this  
 735 cell density (Fig. S10). On the contrary, protocatechuate,  
 736 known to be present in the medium of quinate-degrading  
 737 cells (D'Argenio et al. 1999) is indeed excreted (Fig. S9).  
 738 Moreover, APAH does not behave as secondary metabolite:  
 739 it is not formed at high cell density or during a decrease of  
 740 the growth rate, or after exhaustion of the carbon source  
 741 (Fig. S10).

## 742 4 Conclusion

743 We report here the de novo complete structural elucidation  
 744 of a novel and abundant metabolite in *Acinetobacter baylyi*  
 745 ADP1, APAH, a compound that is not restricted to ADP1.

746 To meet the requirement of 'level 1 identification'  
 747 (according to the Metabolomics Standard Initiative), we  
 748 conducted an extensive analytical study that combined NMR  
 749 and LC/HRMS/MS<sup>n</sup> techniques. Finally, its identity was  
 750 established according to comparison of its retention time,  
 751 MS<sup>2</sup> and <sup>1</sup>H NMR spectra with a synthetic standard. This  
 752 work illustrates the significant effort required to unambigu-  
 753 ously identify a previously unreported metabolite, which still  
 754 remains orphan of enzyme/gene.

755 Interpretation of experimental MS and NMR data for  
 756 metabolite identification is crucial for metabolism interpre-  
 757 tation, but cannot be scaled up to adapt with the hundreds or  
 758 thousands of compounds present in a metabolome. Improve-  
 759 ment of tandem mass spectral libraries and MS/MS scoring  
 760 algorithms are needed (Kind et al. 2018) for faster com-  
 761 pound identification and biochemical landscape covering.

762 To gain insight from APAH biosynthesis, we are actually  
 763 conducting a LC/HRMS-based screening of the collection of  
 764 2600 single-gene deletion mutants of ADP1 (de Berardinis  
 765 et al. 2008). Detecting the mutant metabolomes devoid of  
 766 APAH shall inform us on the genes involved in its formation  
 767 and led us to start reconstituting APAH synthetic pathway.

**Acknowledgements** We thank Jean-François Gallard from Institut de  
 Chimie des Substances Naturelles (CNRS, Gif-sur-Yvette, France) for  
 his expertise in NMR. The authors would like to thank Olek Maciejak  
 and Marie-Jeanne Clément (SABNP, INSERM U 1204—Université  
 d'Evry Val-d'Essonne, Université Paris-Saclay, France) for assistance  
 in <sup>1</sup>H and <sup>13</sup>C NMR experiments. We are grateful to Cécile Robert-  
 Ansart who was involved as part of a student internship in the project.

**Author contributions** MS and AP conceived the study. MT, LS, ED,  
 CL and EP conducted experiments. MT, LS, ED, CL, EP, JCT, PLS and  
 AP analyzed data. MT, ED, JCT, PLS and AP wrote the manuscript.  
 All authors read and approved the manuscript.

**Funding** This work was supported by grants from the Commissariat à  
 l'Energie Atomique et aux Energies Alternatives, CNRS, and Univer-  
 sité Evry-Val-d'Essonne/Université Paris-Saclay, and by the Region Ile  
 de France for financial support of the 600 MHz NMR spectrometer.

## 783 Compliance with ethical standards

**Conflict of interest** All authors declare that they have no conflict of  
 interest.

## 786 References

Aflaki, F., Ghoulipour, V., Saemian, N., & Salahinejad, M. (2014).  
 A simple method for benzoyl chloride derivatization of biogenic  
 amines for high performance liquid chromatography. *Analytical  
 Methods*, 6, 1482–1487.

Afonso, C., Cole, R. B., & Tabet, J. C. (2010) Dissociation of even-  
 electron ions. In Wiley (Ed.), *Electrospray and MALDI mass spec-  
 trometry*. New York: Wiley

Bazile, S., Moreau, N., Bouzard, D., & Essiz, M. (1992). Relation-  
 ships among antibacterial activity, inhibition of DNA gyrase, and  
 intracellular accumulation of 11 fluoroquinolones. *Antimicrobial  
 Agents and Chemotherapy*, 36, 2622–2627.

Bennett, B. D., Kimball, E. H., Gao, M., Osterhout, R., Van Dien, S. J.,  
 & Rabinowitz, J. D. (2009). Absolute metabolite concentrations  
 and implied enzyme active site occupancy in *Escherichia coli*.  
*Nature Chemical Biology*, 5, 593–599.

Bingol, K., Bruschiweiler-Li, L., Li, D., Zhang, B., Xie, M., & Bruschi-  
 weiler, R. (2016) Emerging new strategies for successful metabo-  
 lite identification in metabolomics. *Bioanalysis*, 8, 557–573.

Chang, Y. C., Hu, Z., Rachlin, J., Anton, B. P., Kasif, S., Roberts, R. J.,  
 & Steffen, M. (2016). COMBEX-DB: An experiment centered  
 database of protein function: knowledge, predictions and knowl-  
 edge gaps. *Nucleic Acids Research*, 44, D330–D335.

D'Argenio, D. A., Segura, A., Coco, W. M., Bunz, P. V., & Ornston, L.  
 N. (1999). The physiological contribution of *Acinetobacter* PcaK,  
 a transport system that acts upon protocatechuate, can be masked  
 by the overlapping specificity of VanK. *Journal of Bacteriology*,  
 181, 3505–3515.

de Berardinis, V., Durot, M., Weissenbach, J., & Salanoubat, M. (2009).  
*Acinetobacter baylyi* ADP1 as a model for metabolic system biol-  
 ogy. *Current Opinion in Microbiology*, 12, 568–576.

de Berardinis, V., Vallenet, D., Castelli, V., Besnard, M., Pinet, A.,  
 Cruaud, C., ... Weissenbach, J. (2008). A complete collection  
 of single-gene deletion mutants of *Acinetobacter baylyi* ADP1.  
*Molecular Systems Biology*, 4, 174.

Dias, D. A., Jones, O. A., Beale, D. J., Boughton, B. A., Benheim, D.,  
 Kouremenos, K. A., ... Wishart, D. S. (2016) Current and future

- perspectives on the structural identification of small molecules in biological systems. *Metabolites*, 6(4), 46.
- Domingo-Almenara, X., Montenegro-Burke, J. R., Benton, H. P., & Siuzdak, G. (2018). Annotation: A computational solution for streamlining metabolomics analysis. *Analytical Chemistry*, 90, 480–489.
- Dunn, W., Erban, A., Weber, R. M., Creek, D., Brown, M., Breitling, R., ... Viant, M. (2013a). Mass appeal: Metabolite identification in mass spectrometry-focused untargeted metabolomics. *Metabolomics*, 9, 44–66.
- Dunn, W. B., Erban, A., Weber, R. J. M., Creek, D. J., Brown, M., Breitling, R., ... Viant, M. R. (2013b). Mass appeal: Metabolite identification in mass spectrometry-focused untargeted metabolomics. *Metabolomics*, 9, 44–66.
- Frainay, C., Schymanski, E., Neumann, S., Merlet, B., Salek, R., Jourdan, F., & Yanes, O. (2018). Mind the gap: Mapping mass spectral databases in genome-scale metabolic networks reveals poorly covered areas. *Metabolites*, 8, 51.
- Galperin, M. Y., & Koonin, E. V. (2004). 'Conserved hypothetical' proteins: Prioritization of targets for experimental study. *Nucleic Acids Research*, 32, 5452–5463.
- Hamana, K., & Matsuzaki, S. (1992). Diaminopropane occurs ubiquitously in *Acinetobacter* as the major polyamine. *The Journal of General and Applied Microbiology*, 38, 191–194.
- Horai, H., Arita, M., Kanaya, S., Nihei, Y., Ikeda, T., Suwa, K., Ojima, Y., ... Nishioka, T. (2010). MassBank: A public repository for sharing mass spectral data for life sciences. *Journal of Mass Spectrometry*, 45, 703–714.
- Jimenez, J. I., Minambres, B., Garcia, J. L., & Diaz, E. (2002). Genomic analysis of the aromatic catabolic pathways from *Pseudomonas putida* KT2440. *Environmental Microbiology*, 4, 824–841.
- Kale, N. S., Haug, K., Conesa, P., Jayseelan, K., Moreno, P., Rocca-Serra, P., ... Steinbeck, C. (2016). MetaboLights: An open-access database repository for metabolomics data. *Current Protocols in Bioinformatics*, 53, 14 13 1–18.
- Kanehisa, M., Goto, S., Sato, Y., Furumichi, M., & Tanabe, M. (2012). KEGG for integration and interpretation of large-scale molecular data sets. *Nucleic Acids Research*, 40, D109–D114.
- Kind, T., & Fiehn, O. (2007). Seven Golden Rules for heuristic filtering of molecular formulas obtained by accurate mass spectrometry. *BMC Bioinformatics*, 8, 105.
- Kind, T., & Fiehn, O. (2010). Advances in structure elucidation of small molecules using mass spectrometry. *Bioanalytical Reviews*, 2, 23–60.
- Kind, T., Tsugawa, H., Cajka, T., Ma, Y., Lai, Z., Mehta, S. S., ... Fiehn, O. (2018). Identification of small molecules using accurate mass MS/MS search. *Mass Spectrometry Reviews*, 37, 513–532.
- Levsen, K., Schiebel, H. M., Terlouw, J. K., Jobst, K. J., Elend, M., Preiss, A., ... Ingendoh, A. (2007). Even-electron ions: A systematic study of the neutral species lost in the dissociation of quasi-molecular ions. *Journal of Mass Spectrometry*, 42, 1024–1044.
- Martin, G., & Williams, A. (2008) *Utilizing long-range <sup>1</sup>H-<sup>15</sup>N 2D NMR spectroscopy in chemical structure elucidation*. New York: Wiley.
- Martin, G. E., & Hadden, C. E. (2000). Long-range 1H–15N heteronuclear shift correlation at natural abundance. *Journal of Natural Products*, 63, 543–585.
- Metzgar, D., Bacher, J. M., Pezo, V., Reader, J., Döring, V., Schimmel, P., ... de Crécy-Lagard, V. (2004). *Acinetobacter* sp. ADP1: An ideal model organism for genetic analysis and genome engineering. *Nucleic Acids Research*, 32, 5780–5790.
- Peironcelly, J. E., Rojas-Cherto, M., Fichera, D., Reijmers, T., Coulier, L., Faulon, J. L., & Hankemeier, T. (2012). OMG: Open molecule generator. *Journal of Cheminformatics*, 4, 21.
- Rojas-Cherto, M., van Vliet, M., Peironcelly, J. E., van Doorn, R., Kooyman, M., te Beek, T., ... Reijmers, T. (2012). MetiTree: A web application to organize and process high-resolution multi-stage mass spectrometry metabolomics data. *Bioinformatics*, 28, 2707–2709.
- Roux, A., Lison, D., Junot, C., & Heilier, J. F. (2011). Applications of liquid chromatography coupled to mass spectrometry-based metabolomics in clinical chemistry and toxicology: A review. *Clinical Biochemistry*, 44, 119–135.
- Sawada, Y., Nakabayashi, R., Yamada, Y., Suzuki, M., Sato, M., Sakata, A., ... Saito, K. (2012). RIKEN tandem mass spectral database (ReSpect) for phytochemicals: A plant-specific MS/MS-based data resource and database. *Phytochemistry*, 82, 38–45.
- Siehler, S. Y., Dal, S., Fischer, R., Patz, P., & Gerischer, U. (2007). Multiple-level regulation of genes for protocatechuate degradation in *Acinetobacter baylyi* includes cross-regulation. *Applied and Environmental Microbiology*, 73, 232–242.
- Singh, D. P., Govindarajan, R., Khare, A., & Rawat, A. K. (2007). Optimization of a high-performance liquid chromatography method for the separation and identification of six different classes of phenolics. *Journal of Chromatographic Science*, 45, 701–705.
- Smith, C. A., O'Maille, G., Want, E. J., Qin, C., Trauger, S. A., Brandon, T. R., ... Siuzdak, G. (2005). METLIN: A metabolite mass spectral database. *Therapeutic Drug Monitoring*, 27, 747–751.
- Stuani, L., Lechaplais, C., Salminen, A., Ségurens, B., Durot, M., Castelli, V., ... Perret, A. (2014). Novel metabolic features in *Acinetobacter baylyi* ADP1 revealed by a multiomics approach. *Metabolomics*, 10(6), 1–16.
- Sumner, L. W., Amberg, A., Barrett, D., Beale, M. H., Beger, R., Daykin, C. A., ... Viant, M. R. (2007). Proposed minimum reporting standards for chemical analysis Chemical Analysis Working Group (CAWG) Metabolomics Standards Initiative (MSI). *Metabolomics*, 3, 211–221.
- Tsugawa, H., Kind, T., Nakabayashi, R., Yukihiro, D., Tanaka, W., Cajka, T., ... Arita, M. (2016). Hydrogen rearrangement rules: Computational MS/MS fragmentation and structure elucidation using MS-FINDER Software. *Analytical Chemistry*, 88, 7946–7958.
- van der Hoft, J. J., Vervoort, J., Bino, R. J., Beekwilder, J., & de Vos, R. C. (2011). Polyphenol identification based on systematic and robust high-resolution accurate mass spectrometry fragmentation. *Analytical Chemistry*, 83, 409–416.
- Viant, M. R., Kurland, I. J., Jones, M. R., & Dunn, W. B. (2017). How close are we to complete annotation of metabolomes? *Current Opinion in Chemical Biology*, 36, 64–69.
- Wishart, D. S., Jewison, T., Guo, A. C., Wilson, M., Knox, C., Liu, Y., ... Scalbert, A. (2013). HMDB 3.0—The Human Metabolome Database in 2013. *Nucleic Acids Research*, 41, D801–D807.
- Wolf, S., Schmidt, S., Müller-Hannemann, M., & Neumann, S. (2010). In silico fragmentation for computer assisted identification of metabolite mass spectra. *BMC Bioinformatics*, 11, 148.
- Young, D. M., Parke, D., & Ornston, L. N. (2005). Opportunities for genetic investigation afforded by *Acinetobacter baylyi*, a nutritionally versatile bacterial species that is highly competent for natural transformation. *Annual Review of Microbiology*, 59, 519–551.
- Zhu, Z. J., Schultz, A. W., Wang, J., Johnson, C. H., Yannone, S. M., Patti, G. J., & Siuzdak, G. (2013). Liquid chromatography quadrupole time-of-flight mass spectrometry characterization of metabolites guided by the METLIN database. *Nature Protocols*, 8, 451–460.

**Publisher's Note** Springer Nature remains neutral with regard to jurisdictional claims in published maps and institutional affiliations.

Journal:	<b>11306</b>
Article:	<b>1508</b>

## Author Query Form

**Please ensure you fill out your response to the queries raised below and return this form along with your corrections**

Dear Author

During the process of typesetting your article, the following queries have arisen. Please check your typeset proof carefully against the queries listed below and mark the necessary changes either directly on the proof/online grid or in the 'Author's response' area provided below

Query	Details Required	Author's Response
<a href="#">AQ1</a>	Author: The affiliation '3' has been split into two different affiliations '3 and 4'. Please check, and correct if necessary.	
<a href="#">AQ2</a>	Author: Kindly check and confirm all affiliations.	
<a href="#">AQ3</a>	Author: Reference de Berardinis (2009) was cited in text but not provided in the reference list. Please provide reference in the list or delete the citation.	
<a href="#">AQ4</a>	Author: As per the information provided by the publisher, Fig. 1 will be black and white in print; hence, please confirm whether we can add "colour figure online" to the caption.	